CONTENTS

1. P.B. Wilson, "Mode Impedances for PEP- and PETRA-Type Cavities" LEP-70/69, May 1978.

2. Table 1. Identical to Table 1 in the above reference except that the values were obtained by URMEL and not, as in the above reference, by SUPER-FISH.

3. Table 2. A list of dipole PEP cavity parameters obtained with URMEL. There is no equivalent table in Ref. 1, as SUPERFISH works only with monopole modes.

4. A sketch of the cavity as input to URMEL. Note the slight difference between these dimensions and the ones given in Ref. 1.

STANFORD UNIVERSITY

STANFORD LINEAR ACCELERATOR CENTER
ACCELERATOR PHYSICS

Mail Address:
Z. D. Farkas, Bin 22
SLAC, P.O.Box 4349
Stanford, California, 94305
(415) 854-3300 ext. 3387

September 26, 1985

Swapan Chattopadhyay
MS-90-4040
Lawrence Berkely Laboratory
Berkely, CA 94720

Dear Dr. Chattopadhyay

Enclosed find the following:

1. P. B. Wilson, "Mode Impedances for PEP- and PETRA-Type Cavities" LEP-70/69, May 1978.
2. Table 1. Identical to Table 1 in the above reference except that the values were obtained by URMEL and not, as in the above reference, by SUPERFISH.
3. Table 2. A list of dipole PEP cavity parameters obtained with URMEL. There is no equivalent table in reference 1, as SUPERFISH works only with monopole modes.
4. A sketch of the cavity as input to URMEL. Note the slight difference between the these dimensions and the ones given in reference 1.

Let me know if you require any further clarification. The copious URMEL outputs are here at SLAC. URMEL was run by K. Bane.

Sincerely,

Z. David Farkas

Z. David Farkas

LEP-70/69

17.5.1978

MODE IMPEDANCES FOR PEP- AND PETRA-TYPE CAVITIES

P.B. Wilson

The impedance of the RF cavities will dominate the impedance of the LEP ring. Fortunately, the impedances of the fundamental and higher-order cavity modes can be computed with fair accuracy using SUPERFISH. Results are given in this note for both a PEP-type cavity (30° nose cone angle) and a PETRA-type cavity (60° nose cone angle) having a beam aperture radius of 5.0 cm. The dimensions of the two cavities are shown in Fig. 1.

Tables I and II give the frequencies, R/Q's, unloaded Q's and values of the loss parameter k for all the modes computed for the two cavities. It is probable that all the modes below the cut-off frequency (2295 MHz) of the beam pipe have been found. At least, there is a one-to-one correspondence between modes in the two cavities in terms of their parity; that is, the interlacing of even and odd modes is the same. A further attempt was made to categorize the mode type by means of the four indices listed in the first column of Tables I and II. The first two indices give the number of reversals in the magnetic field (H_{ϕ}) between the cavity axis and the outer (top) boundary, counting the reversal on the axis. The first index gives the number of reversals along the left boundary, and the second the number of reversals along the symmetry plane. The two indices following the comma give the number of field reversals along the top boundary and along the axis respectively for the full cavity. Thus the sequence of the indices is LS,TA where S is also the right boundary for a half-cavity run. Note that most of the modes are "hybrid" modes, in the sense that they seem to be mixtures of the pure normal modes for a pillbox cavity. For example, no pure TM_{020} (22,00) or TM_{012} (11,22) modes were found. Mode number 3, however, seems to be a mixture of these two modes. Perhaps the perturbation due to the addition of a nose cone to a pillbox shifts the frequencies of the two pure modes so that they cross.

In the case of the PETRA cavity, there is some ambiguity in mode identification because there is not a sharp dividing point between the left and top boundaries (see Fig. 1). When a field reversal occurs along the slanted corner surface, the mode can be counted in two ways, depending on the exact point chosen to mark the dividing point between the left and top boundaries.

Alternative ways of categorizing the mode are indicated in parentheses in Table I for such cases. Sketches showing the field patterns for the first nine higher-order modes in the PETRA cavity are given in Fig. 2.

Problems were experienced with the Q calculation in SUPERFISH, for some modes, especially in the case of the PETRA cavity. For example, in modes 10, 11 and 12 the program was run twice, the first time with the driving point in the upper left corner, and the second time with the driving point in the upper right corner (on the plane of symmetry). Computed values of frequency and R/Q agreed closely between the two runs, but the Q's for mode 10 were different by nearly a factor of two. In the case of mode 16, the run was made twice with identical parameters, but two very different results were obtained for Q. The Q value for mode 13 seems out of line compared to the Q value for the corresponding PEP mode. Until these ambiguities in the Q calculations in SUPERFISH have been resolved, the Q value listed in the Tables, at least for the higher frequency modes, should not be accepted uncritically.

The loss parameter k is given in Fig. 3 as a function of bunch length for the two cavities. Here k_o is the loss to the fundamental mode in the single pass limit, and k_{hom} is the loss to all other modes. The results have been corrected for modes with frequencies greater than 2600 MHz (the limit of the SUPERFISH calculation) using KN7C, as described in LEP-70/41. The correction to k_{hom} was 18% at σ_z = 1.5 cm and 5% at σ_z = 2.5 cm. Within the errors of the calculations, we note that k_{tot} and k_{hom} are nearly the same for the two cavities.

Since the PETRA cavity is of more interest for LEP, the higher-mode loss impedance per cell, Z_{hm} (cell), and the beam loading enhancement factor B are plotted as a function of bunch length for this cavity in Fig. 4. For an RF structure of 3200 cells (L = 1344 m), the loss impedance to higher order modes is Z_{hm} (RF) = 11.8 GΩ at σ_z = 2.5 cm. Adding on 4.7 GΩ for the remaining vacuum chamber impedances as computed in LEP-70/41, the total parasitic mode loss impedance and the parasitic mode energy loss per turn become

$$Z_{pm} = 16.5\ \text{G}\Omega \qquad (\sigma_z = 2.5\ \text{cm})$$

$$V_{pm} = 173\ \text{MV} \qquad (I_o = 10.5\ \text{mA})$$

It is of interest also to compare the parameters of the two cavities for the fundamental mode. By the increasing of the outer radius of the PETRA cavity to 302 mm (see Fig. 1), the frequency of the fundamental mode is lowered to 357.0 MHz. The parameters for this cavity are compared with those for the PEP cavity in the table below.

		PETRA	PEP
Frequency	(MHz)	357.0	357.3
R/Q	(ohms)	251.0	271.3
Q_o		47,250	44,300
R	(MΩ/cell)	11.86	12.02
r	(MΩ/m)	28.25	28.62

It is seen that the shunt impedances per unit length are nearly the same for the two cavities.

Assuming a reduction in unloaded Q by 15%, due to coupling slots and surface imperfections, we obtain the parameters listed below for the PETRA cavity.

PETRA Cavity Parameters at 85% Q_o

Q_o	(85%)	40,165
R	(MΩ/cell)	10.08
r	(MΩ/m)	24.01
T_{fo}	(μs)	35.8
τ_o		0.517

Here T_{fo} is the unloaded filling time, and τ_o the ratio of the bunch passage time (18.52 μs) to T_{fo}. For a structure with a total length of 1344 m (3200 cells), the total shunt impedance is 32.26 GΩ.

TABLE I
PETRA Cavity Modes

Mode Number and Type	Frequency (MHz)	R/Q (ohms)	Q_0 ($\times 10^{-3}$)	k (V/pC)
1 Even 11,00	359.2	250.4	47.2	.1413
2 Odd 11,11	525.0	55.6	40.5	.0458
3 Even 21,20	886.5	9.4	71.5	.0130
4 Odd 22,11	974.0	44.2	26.1	.0677
5 Even 22,22	1221.1	17.0	39.8	.0327
6 Odd 21,31	1237.4	4.1	26.5	.0080
7 Even 33,00	1396.0	7.7	99.5	.0168
8 Odd 32,31	1466.1	2.3	24.6	.0054
9 Odd 22,33	1564.8	5.5	20.9	.0134
10 Even 21,42 (31,22)	1588.0	6.6	38.2 (68.5)	.0165
11 Even 32,42	1700.6	4.6	71.4 (66.7)	.0123
12 Even 33,40 (43,20)	1854.7	1.9	— (59.9)	.0054
13 Odd 43,31	1888.3	4.3	71.4 ?	.0129
14 Even 24,40	1931.5	0.2	108.5	.0007
15 Odd 44,11	1990.3	6.6	23.4	.0206
16 Odd 12,53	2035.5	1.4	18.1 (70.4)	.0045
17 Even 43,42	2107.3	0.3	72.8	.0011
18 Odd 32,31	2220.0	0.4	70.2	.0016
19 Even 34,42 (44,22)	2261.2	6.2	78.2	.0219
Cutoff Frequency	(2295)			
20 Odd 43,53	2355.4			.0030
21 Even	2372.3			.0002
22 Even	2416.9			.0005
23 Odd	2429.2			.0012
24 Even	2492.2			.0036
25 Even	2558.8			.0001
26 Odd	2587.6			.0002

Figure 2

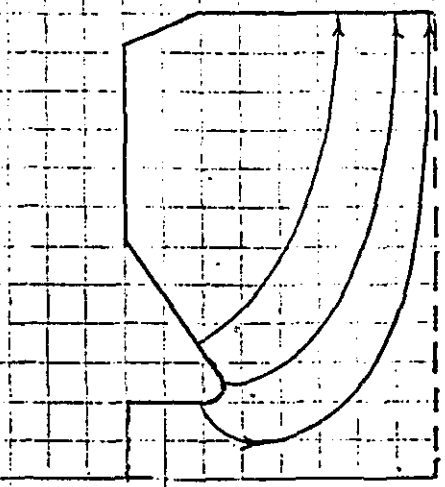

2

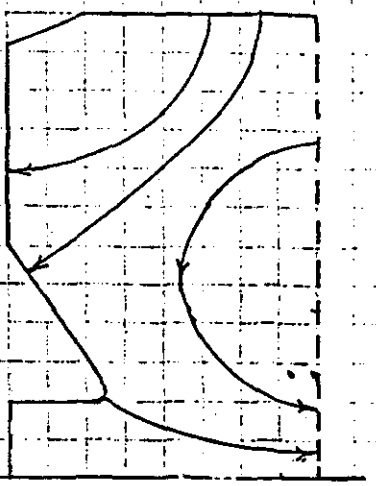

3

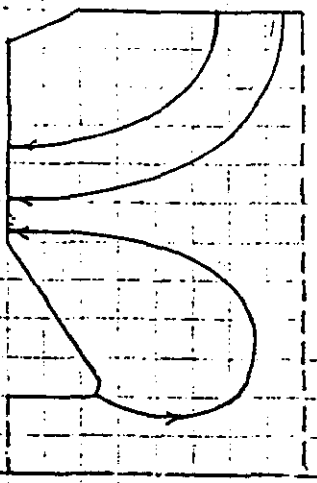

4

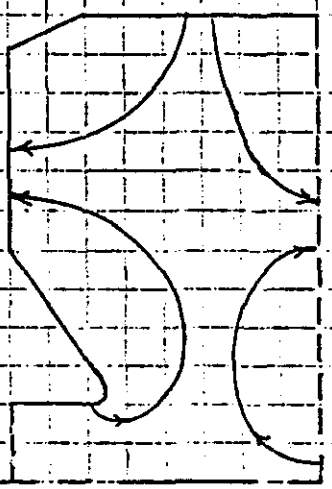

5

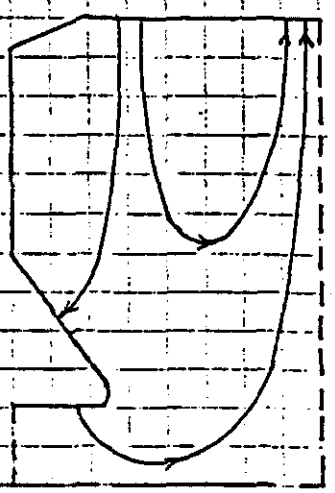

6

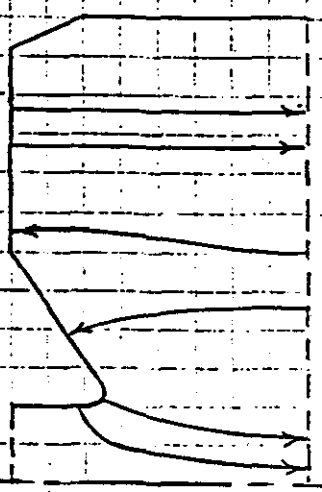

7

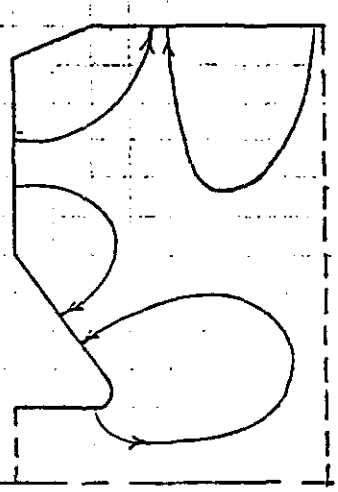

8

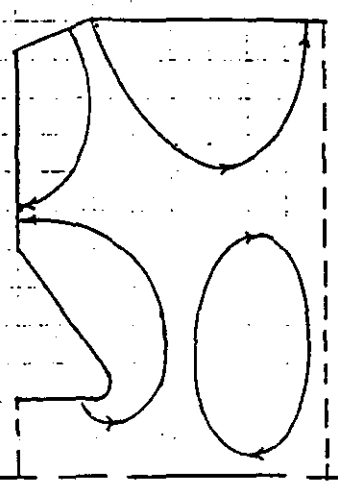

9

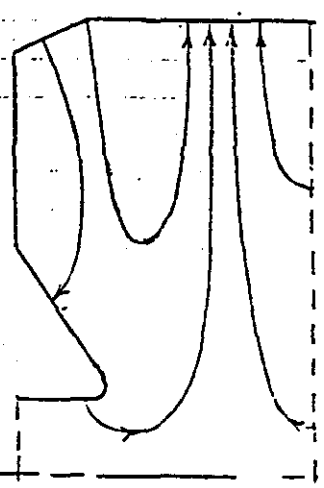

10

Figure 3

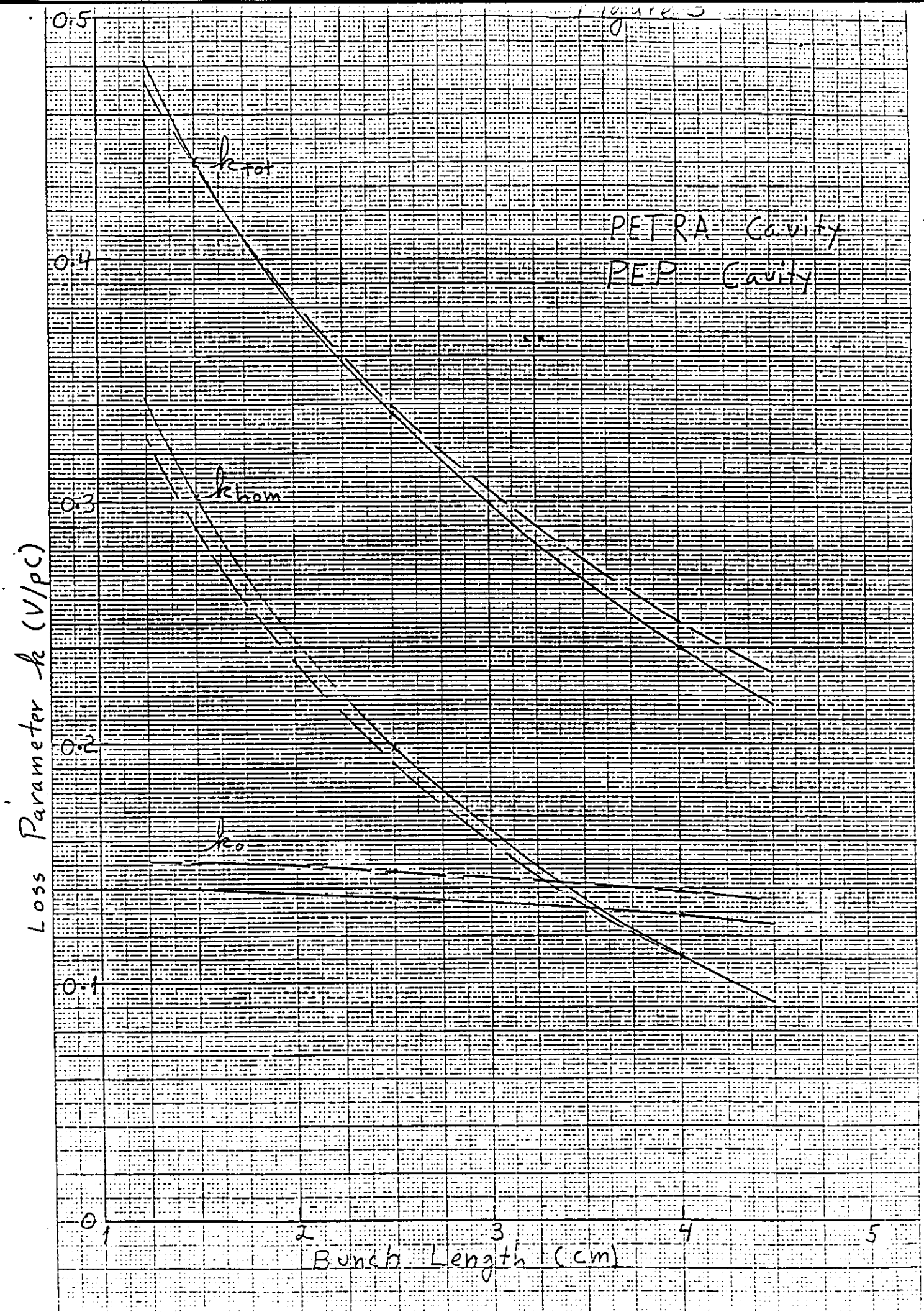
0.5
0.4
0.3
0.2
0.1
0
1
2
3
4
5
k_{tot}
k_{hom}
k_0
PETRA Cavity
PEP Cavity
Loss Parameter k (V/pC)
Bunch Length (cm)

TABLE II

PEP Cavity Modes

Mode Number and Type			Frequency (MHz)	R/Q (ohms)	Q_0 ($\times 10^{-3}$)	k (V/pC)
1	Even	11,00	357.3	271.3	44.3	.1523
2	Odd	11,11	510.2	60.4	37.6	.0484
3	Even	21,20	875.9	10.7	55.9	.0148
4	Odd	22,11	912.3	43.5	20.6	.0623
5	Even	22,22	1158.5	14.1	51.7	.0257
6	Odd	21,31	1222.6	4.3	62.3	.0083
7	Even	33,00	1416.0	3.8	54.5	.0084
8	Odd	32,31	1447.8	8.6	22.2	.0195
9	Odd	33,11	1501.3	0.4	17.5	.0009
10	Even	21,42	1597.3	3.4	39.0	.0086
11	Even	33,22	1644.8	4.3	28.9	.0112
12	Even	32,42	1777.2	7.1	60.2	.0198
13	Odd	43,31	1838.4	0.8	16.5	.0022
14	Even	24,00	1949.2	0.1	131.0	.0003
15	Odd	21,53	1974.7	3.0	20.3	.0093
16	Odd	32,53	2055.2	5.9	18.9	.0191
17	Even	43,42	2070.8	1.1	71.7	.0034
18	Odd	42,51	2150.1	1.9	76.9	.0063
19	Even	44,22	2263.3	2.0	61.0	.0069
Cutoff Frequency			(2295)			
20		43,53	2320.9			.0028
21			2365.2			.0017
22			2390.8			.0042
23			2402.7			.0004
24			2483.2			.0089
25			2515.4			.0001
26			2547.1			.0000
27			2585.0			.0023

Figure 1

PETRA Cavity

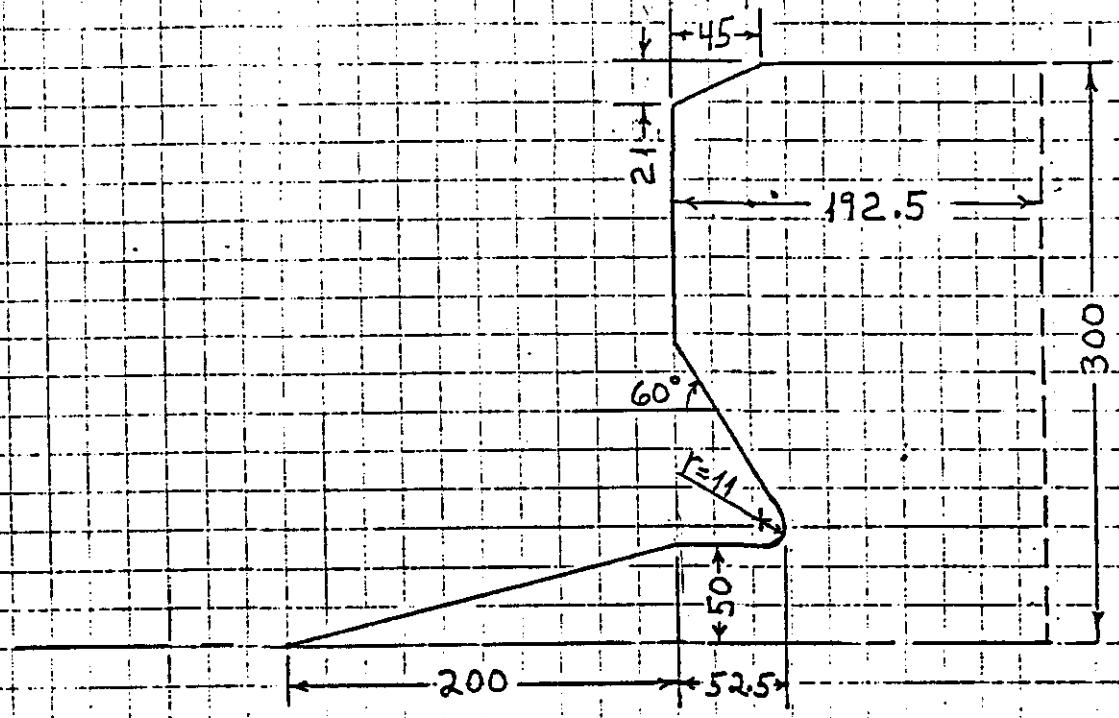

PEP Cavity

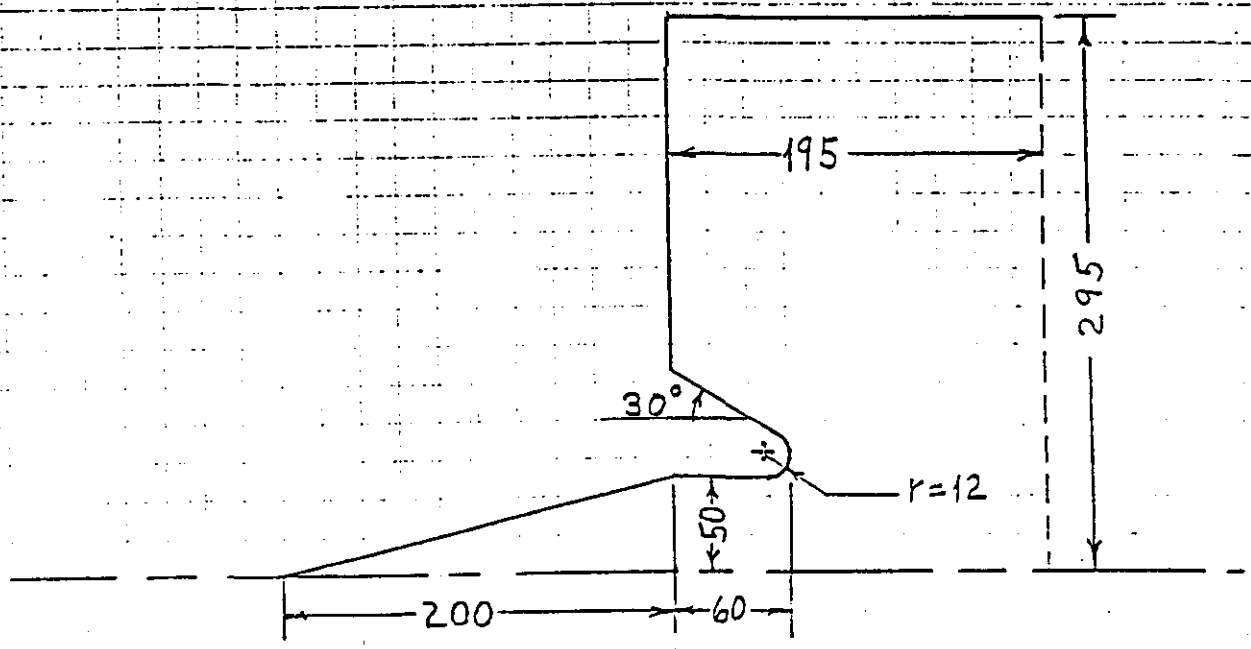

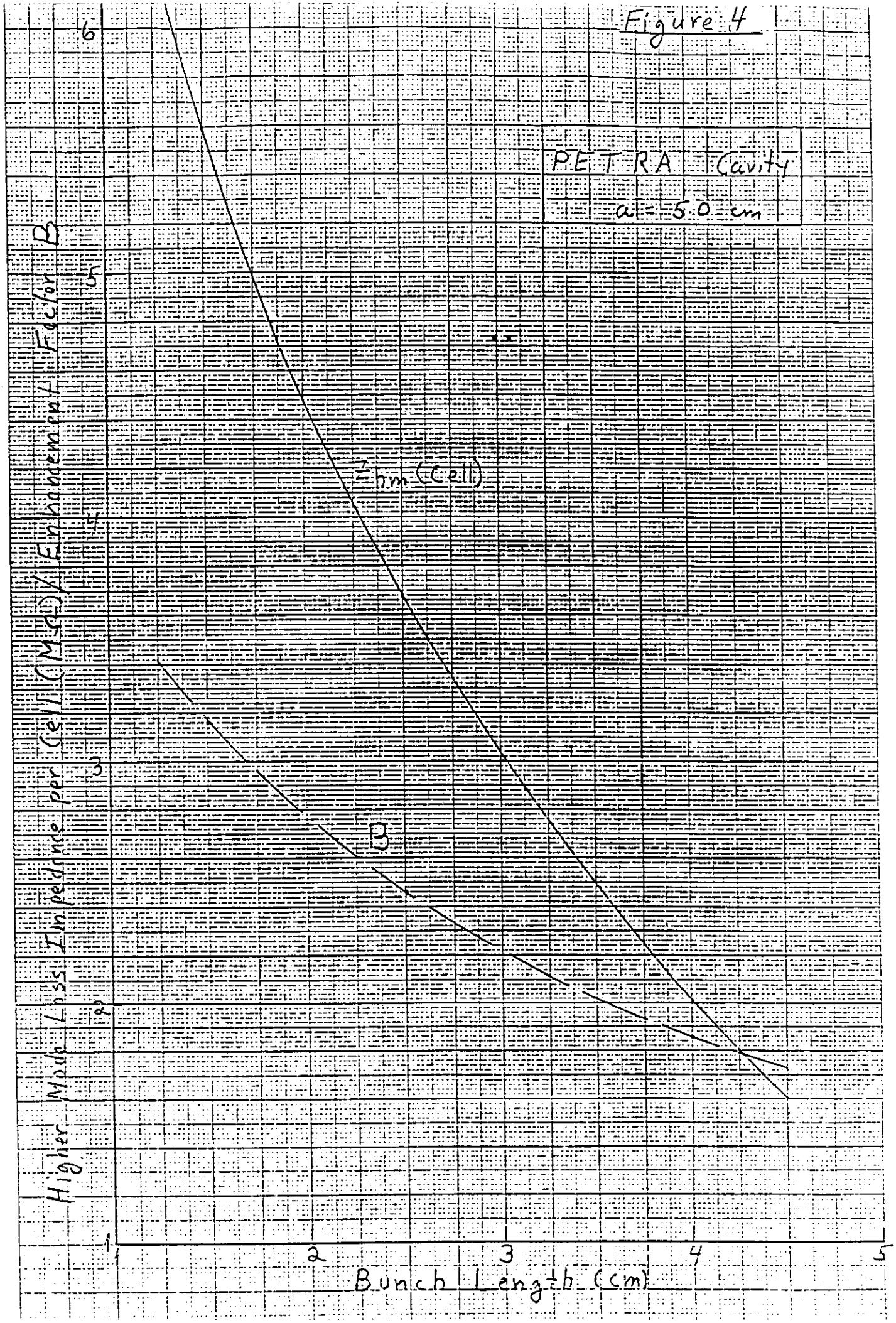
Figure 4
PETRA Cavity
a = 5.0 cm
Higher Mode Loss Impedance per Cell (MΩ)/Enhancement Factor B
Bunch Length (cm)
Z hm (Cell)
B
1
2
3
4
5
6

Table 1. MONOPOLE PEP CAVITY MODES (from URMEL)

PBW number	Mode	Frequency (MHz)	R/Q (ohms)	Q (x 10^{-3})	k (V/pC)
1	EE-1	358.9	276	42.9	.1551
2	MM-1	507.2	55.6	36.5	.0443
*	EE-2	830.2	.572	44.4	.0163
3	EE-3	883.4	9.76	54.5	.0135
4	MM-2	926.1	41.4	35.8	.0603
5	EE-4	1167.1	12.3	50.6	.0412
6	MM-3	1215.7	5.36	61.9	.0102
7	EE-5	1440.1	4.74	91.5	.0107
8	MM-4	1447.4	9.14	60.7	.0207
9	MM-5	1533.0	.342	53.5	.0008
10	EE-6	1586.0	3.36	70.8	.0085
11	EE-7	1668.5	5.10	55.3	.0134
12	EE-8	1737.7	5.30	56.3	.0148
13	MM-6	1852.2	.292	58.3	.0085
14	MM-7	1958.9	3.88	77.8	.0119
15	EE-9	1971.6	—	—	—
16	MM-8	2065	11.1	71.5	.0359
17	EE-10	2077	1.80	72.1	.0006
18	MM-9	2153	.550	83.6	.0019
19	EE-11	2290	1.68	68.9	.0060

* missed by SUPERFISH

— not given by URMEL

$$R/Q = \frac{V^2}{\omega U} \quad , \quad k = \frac{V^2(r=0)}{4U}$$

V is the accelarating voltage and U is the energy stored in the cell.

Table 2. DIPOLE PEP CAVITY MODES (from URMEL)

Mode number	Frequency (MHz)	$(R/Q)_t$ (ohms)	$(R/Q)_t^*$ (ohms)	Q (x 10^{-3})	k (V/pC)
MM-1	506	.869	3.08	47.1	.0014
EE-1	633.8	9.65	21.8	62.7	.0019
MM-2	774.4	14.5	21.9	48.5	.0352
EE-2	851.1	.368	.461	52.4	.0010
MM-3	967.4	.118	.114	98.4	.0036
EE-3	1047	.0956	.079	48.5	.0030
EE-4	1091	5.21	3.97	62.8	.0180
MM-4	1094	16.9	12.8	41.5	.0582
EE-5	1222	.941	.571	84.2	.0036
MM-5	1243	2.75	1.61	59.3	.0107
EE-6	1367	14.2	6.88	67.3	.061
MM-6	1393	.059	.028	81.9	.0003
MM-7	1463	.078	.033	141	.0004
MM-8	1527	—	—	—	—
EE-7	1604	.2496	.084	70.0	.0013
MM-9	1606	5.21	3.97	62.8	.0230
EE-8	1642	.249	.084	108	.0013
MM-10	1697	3.60	1.13	63.5	.0500

$$(R/Q)_t = \frac{V^2(r=a)}{2\omega U} \quad , \quad (R/Q)_t^* = (R/Q)_t \times k^2 a^2 \quad , \quad k_t = \frac{V^2(r=a)}{4U}$$

V is the accelarating voltage, U is the energy stored in the cell, k is the wavenumber and a is the aperture radius.

PEP CAVITY HALF CELL

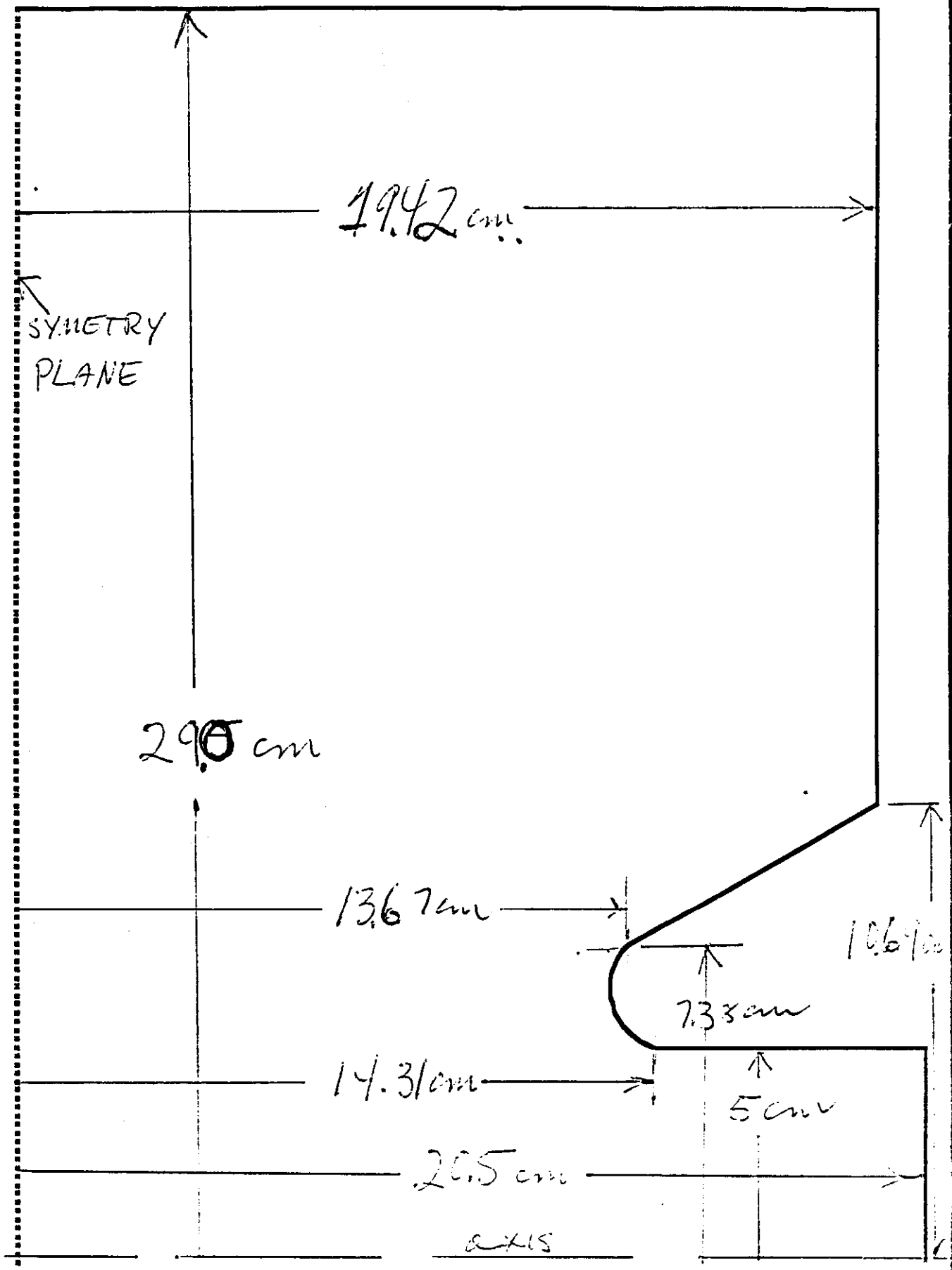

FRAME= 1

TEXT:PEP000-PEP CAVITY; ZERO MODE : ID:PEP0EE 7:16:45

PLOT:CAVITY SHAPE